



Cite this: *Lab Chip*, 2017, 17, 2693

## Integration and application of optical chemical sensors in microbioreactors

Pia Gruber, <sup>a</sup> Marco P. C. Marques, <sup>a</sup> Nicolas Szita <sup>\*a</sup> and Torsten Mayr <sup>\*b</sup>

The quantification of key variables such as oxygen, pH, carbon dioxide, glucose, and temperature provides essential information for biological and biotechnological applications and their development. Microfluidic devices offer an opportunity to accelerate research and development in these areas due to their small scale, and the fine control over the microenvironment, provided that these key variables can be measured. Optical sensors are well-suited for this task. They offer non-invasive and non-destructive monitoring of the mentioned variables, and the establishment of time-course profiles without the need for sampling from the microfluidic devices. They can also be implemented in larger systems, facilitating cross-scale comparison of analytical data. This tutorial review presents an overview of the optical sensors and their technology, with a view to support current and potential new users in microfluidics and biotechnology in the implementation of such sensors. It introduces the benefits and challenges of sensor integration, including, their application for microbioreactors. Sensor formats, integration methods, device bonding options, and monitoring options are explained. Luminescent sensors for oxygen, pH, carbon dioxide, glucose and temperature are showcased. Areas where further development is needed are highlighted with the intent to guide future development efforts towards analytes for which reliable, stable, or easily integrated detection methods are not yet available.

Received 18th May 2017,  
Accepted 7th July 2017

DOI: 10.1039/c7lc00538e

rsc.li/loc

<sup>a</sup> Department of Biochemical Engineering, University College London, Gower Street, WC1E 6BT, London, UK. E-mail: n.szita@ucl.ac.uk;

Tel: +44 (0)20 7679 9814

<sup>b</sup> Institute of Analytical Chemistry and Food Chemistry, Graz University of Technology, Stremayrgasse 9, 8010 Graz, Austria. E-mail: torsten.mayr@tugraz.at; Tel: +43 316 873 32504

## 1. Introduction

Since their first inception in the 1980s when Lübbers *et al.*<sup>1</sup> and Wolfbeis *et al.*<sup>2</sup> demonstrated the oxygen quenching of various fluorescent dyes immobilized in silicone membranes,



Pia Gruber

Pia Gruber is currently working at University College London as a PhD student and Marie Curie Trainee of the EUROMBR Initial Training Network in the research group of Professor Nicolas Szita. Her main research interests are biocatalysis, micro-scale sensor technology, chemo-enzymatic, and enzymatic reaction cascades. Previously, Pia graduated with honors from the Graz University of Technology (TUG) with an MSc degree in Chemistry.

Her master thesis topic was the development of carbon dioxide sensors for marine applications.



Marco Marques

Marco Marques obtained his PhD in Biotechnology at the Instituto Superior Técnico (IST) in Lisbon, Portugal, focusing on the application of small-scale devices to carry out steroid bioconversions. During his post-doc at the Institute of Biotechnology and Bioengineering (Lisbon, Portugal) he established the use of marine bacteria to produce secondary metabolites before joining Professor Nicolas Szita's group at the Department of Biochemical Engineering (UCL). He is working in close collaboration with Sigma Aldrich (Member of Merck Group) and other companies to implement microreactor technologies in bio-based manufacturing processes.

chemical Engineering (UCL). He is working in close collaboration with Sigma Aldrich (Member of Merck Group) and other companies to implement microreactor technologies in bio-based manufacturing processes.



optical sensors have gained popularity due to their typically low cost, compact size, and capability to monitor analytes in a non-invasive fashion. Optical sensors for oxygen are widely applied nowadays and feature in environmental monitoring, bioprocess monitoring,<sup>3</sup> and in life sciences.<sup>3,4</sup> Optical sensors also played a crucial role in establishing new fields: on-line and *in situ* detection of process variables from microliter volumes was at the heart of the successful development of miniaturized and micro(fluidic) bioreactors.<sup>5,6</sup>

In the wake of the success of optical sensors for oxygen, sensors for other analytes relevant for bioprocess monitoring were researched and developed. Using other luminescence principles, sensors to detect the pH, the concentration of glucose and carbon dioxide, and temperature have now been successfully realised. The sensors can be employed either as single analyte detection units or as multi-parametric detection units. Even multiple parameters in one sensor are now possible.<sup>7</sup> The quantification of key variables of biotechnological processes is thus feasible with optical sensors alone. Furthermore, not only have new analytes been added, there is now also a range of novel dyes and sensor matrices, and with it a host of sensor preparation and integration methods. The interested user has thus nowadays a large set of options at hand to tailor optical sensing to their application's needs.

Optical sensors are in many ways ideally suited for microfluidic applications in biology and biotechnology. The small footprint allows integration in small channels, and optical sensing offers *in situ*, non-invasive and non-destructive monitoring which does not interfere with cell metabolism or culture environment. For oxygen sensors, and in contrast to their electro-chemical counterparts,<sup>8</sup> oxygen optical sensors do not consume oxygen. For carbon dioxide sensing, the Severinghaus electrode<sup>9</sup> is difficult to adapt and integrate to microfluidic feature sizes. With optical sensors, the detection

unit does not have to be mechanically coupled with the device (as opposed to electrodes and their wires). This promotes flexibility in the design and operation of a microfluidic device, which has made optical sensors a preferred choice for many microfluidic devices.<sup>10,11</sup>

In this tutorial review, we present an overview of optical sensor-based monitoring options in microfluidic devices. We explain the different sensor formats and fabrication techniques, and discuss their advantages and disadvantages for microfluidic device integration. The working principles of the different detection methods are shown and discussed in the context of applications. Specific examples of oxygen, pH, carbon dioxide, glucose and temperature monitoring are offered to clarify the concepts. Furthermore, they showcase the successful application of optical sensors in microfluidic devices, thereby inspiring both the novice in the field as well as experienced users to find novel monitoring solutions for their applications. We also highlight areas where further improvement and development are required to overcome existing challenges and limitations both in analyte type and detection capabilities. This tutorial review focusses on all the practical aspects and common issues that arise during sensor integration and describes the, at times iterative, path towards attaining a robust read-out of the sensor in the microfluidic device, starting from choices in reactor material and sensor matrices to considerations that should be made before and during the integration and assembly of the system such as bonding and detection methods (Fig. 1).

## 2. Optical sensor formats

The format of a sensor determines the final state in which it is integrated into the microfluidic device. Ideally, sensors should be small, inexpensive to produce, selective to a single



Nicolas Szita

*Nicolas Szita is a Professor of Bioprocess Microfluidics at the Department of Biochemical Engineering, University College London (UCL), UK. He received his Masters degree in Mechanical Engineering and his doctorate degree from the ETH Zurich, Switzerland. He spent his post-doctorate years at MIT, USA, in the group of Professor Klavs Jensen, and was an Associate Professor at DTU, Denmark before joining UCL. His research*

*focusses on the application of microfluidics and microfabricated devices integrated with novel analytical approaches for biological systems and bioprocessing.*



Torsten Mayr

*Torsten Mayr received his PhD in chemistry from the University of Regensburg (Germany) in 2004. In 2002–2004 he was a post-doctoral fellow at the Karolinska Institute in Stockholm (Sweden). Since 2004 he is Assistant Professor at the Institute of Analytical Chemistry and Food Chemistry at the Graz University of Technology. Since 2014 he is Associate Professor the same institute. His research is dedicated to optical chemical*

*sensors and their application in biotechnology and environmental analyses. Further research activities include optical spectroscopy, luminescent materials and the integration of sensors in microfluidic systems.*





**Fig. 1** Flow diagram describing the path towards robust sensor integration in a microfluidic device. The choice of dye is dependent on the expected analyte range, which can also affect the sensor material. Depending on the analyte of interest, different sensing schemes and formats are available; different sensor formats enable integration with different geometries or device materials, which in turn influence the choice of bonding and detection methods. The integration path is iterative. Required bonding methods, e.g. heat-assisted bonding, will exclude certain sensing schemes and thus require an adaptation of the sensor integration. More specific points for each of the main aspects in the boxes of the flow diagram are listed below the diagram.

analyte, have a short response time and user-friendly to the extent that the sensor can be used without time-consuming or complex calibration or setup.<sup>12</sup> Other aspects are long-term stability and limit of detection which are more application dependent. Additionally, a sensor should be able to continuously monitor the analyte, in real time, and without disrupting the reaction or the culture.

Monitoring can either happen online (which is often synonymous with in-line and *in situ* for microfluidic devices) or at-line. Online implies that the sensors: must be integrated inside the microfluidic device; be in direct con-

tact with the liquid; their signal must be read out in real-time; and in an automated manner (whereas in-line can entail manual or discontinuous, non-automated readout). At-line implies that measurements are taken outside of the liquid stream (after which the sample can be returned into the main stream if required). With online monitoring it is possible to obtain continuous time-course data as opposed to data at discrete time points (at-line) or at the end of a process (off-line). The benefits of online monitoring compared to at-line and offline analysis are summarized in Table 1.

**Table 1** Summary of advantages and disadvantages of the different monitoring modes in microfluidic systems

| Summarized | Advantages   | Disadvantages   |
|------------|--|---|
| On-line    | <ul style="list-style-type: none"> <li>- Real time analysis possible</li> <li>- Rapid feedback allows real time process control</li> <li>- No manual sampling required</li> <li>- Measurement at real temperature</li> <li>- No sampling required</li> <li>- Less risk of contamination</li> <li>- Production flow undisturbed by sampling or redirecting</li> </ul> | <ul style="list-style-type: none"> <li>- Possible interaction of sensors with the flow or reactants</li> <li>- Sensors need to be recalibrated and replaced over time</li> <li>- Increase of system complexity (fabrication, design, operation, maintenance)</li> <li>- Cross sensitivity with other analytes or interferences can be difficult to quantify</li> <li>- Limitation to a specific analytical problem and a certain concentration range</li> </ul> |
| At-line    | <ul style="list-style-type: none"> <li>- Significant number of assays/analytical methods available</li> <li>- Can be cost-efficient</li> <li>- Flow cells available</li> <li>- Feedback available quickly</li> </ul>   | <ul style="list-style-type: none"> <li>- Changes in sample before analysis possible</li> <li>- Analysis limited to on-site equipment</li> <li>- Certain sample volume necessary/consumed</li> <li>- Risk of contamination through sampling</li> </ul>   |
| Off-line   | <ul style="list-style-type: none"> <li>- Versatile component analysis possible through instrumental analytical tools (LC/GC/MS)</li> <li>- Variety of analytes can be monitored with one analytical method</li> <li>- Availability of analytical methods with high selectivity and accuracy</li> </ul>   | <ul style="list-style-type: none"> <li>- Slow feedback - Results not in real-time</li> <li>- Risk of contamination through sampling</li> <li>- Sample degradation possible</li> <li>- Analysis at the end of process line</li> </ul>  |



Concerning integration in microfluidic devices, it is important to ensure sufficient signal strength of the sensors, transparency of the selected device materials for the required wavelength range, a high immobilisation stability (if the sensor is immobilised on a surface), no interference with the sample, and preferably an easy way to calibrate the sensor after sensor integration. For biological and biotechnology applications, additionally, the integrated sensors need to be biocompatible and non-toxic to cells and enzymes, and offer ease of sterilization. It may not be possible to fulfil all attributes with one sensor format. Therefore, when a sensor is fabricated, the aim is to achieve as many of the desired characteristics as possible and, ultimately, to create a sensor that is suitable for the application. In the following sections, we describe some of the most common sensor formats available for microfluidic device integration.

### a. Dissolved indicators

Dissolved indicator dyes are the most easily realized monitoring option in terms of the complexity of integration. The dye is dissolved in the reaction media and pumped into the reactor together with the reagents providing an instantaneous response (Fig. 2, a). However, this means that the indicator is present in the product stream and requires an additional recovery steps to separate dye from the product. The possibility of an interaction between indicator and reactants is critical (*i.e.* influencing the response, inactivation or inhibition of an enzyme or toxicity towards cells). The application of these dyes can be difficult when compared to their use in a batch system or a simple cuvette. This is due to the shorter optical path lengths yielding insufficient signal for detection. However, the most straightforward way of increasing the concentration of the indicator to achieve a necessary signal is often not possible because many types of dyes form aggregates, which leads to inhomogeneity and makes the readout

unreliable. An example application where dissolved indicator dyes offer an advantage over other formats is the quantification of a spatial pH gradient lateral to the flow direction inside a channel.<sup>13</sup> To achieve this, a completely homogeneous distribution of the pH indicator dye was required, together with an unchanged background for the entire measurement time.<sup>14–16</sup> Note that if the actual reaction mixture is more turbid than the conditions with which the calibration was established, inaccuracies in the readout will occur.

### b. Sensor layers and spots

A sensor that remains stationary in the microfluidic device is normally preferable for biological or biotechnology applications, as it removes the need to separate indicator dye out of the sample stream, and minimises sensor-sample interaction. To keep them stationary, the sensor dyes are usually embedded in a polymer matrix, either through entrapment or covalent bonding. The requirements for such a polymer are selective permeability towards the analyte and low or no permeability to other components in the sample. The polymer should obviously also not interact with the analyte. In most cases, the indicator dye is embedded in a lipophilic or hydrophilic host polymer, depending on the analyte, to allow them to interact with the sample. To avoid leaching of the sensor material, the dye is either covalently bound to the polymer, or lypophilized by synthetic modification.

A popular format of stationary sensor integration is sensor layers (Fig. 2 b and c). Sensor layers enable analyte detection at different positions of the channel, or the imaging of a larger area to visualize gradients in channel direction. Methods of sensor layer integration include photopolymerization, screen-printing techniques, spray-coating, spin-coating, or gluing of pre-coated sensor foils (these methods will be explained in greater detail in section 3). Spray-coating is performed directly on the surface of a channel wall, while spin coating involves the embedding of the sensor dye into a polymer that is then spun into a thin film on a rotating plate. The resulting film requires a further structuring step to attain the desired sensor size, the cut out sensor spot then needs to be attached in the microfluidic device. Both these processes happen typically before assembly of the device. This means that the device bonding can affect the properties of the sensor dye and the polymer it is embedded in, which in turn can affect sensor performance. Effects might include change of response characteristics, signal loss, or even decomposition of the sensor material. The use of adhesive tape or thermal bonding can lead to the deactivation of sensor materials due to solvents in the adhesive tapes and thermal degradation<sup>17</sup> (bonding methods will be discussed in more detail in section 4). To circumvent some of these issues, sensor integration was demonstrated by physical absorption of dyes or particles onto the surface of an already bonded device. Lasave *et al.*<sup>18</sup> for example successfully demonstrated the formation of a sensing layer through oxygen-sensitive nanoparticle adsorption onto a powder-blasted glass surface.

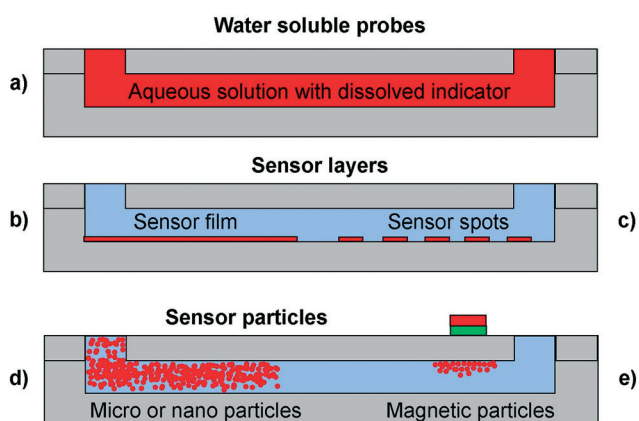


Fig. 2 Sensor formats in microfluidic reactors (gray): a) dissolved indicator dye in the entire channel (red) b) sensor layer in the form of a homogeneous film (red) c) sensor layer in the form of sensor spots d) free sensor particles and e) magnetic sensor particles. The liquid phase is represented in blue. Adapted from Sun *et al.* (2015).<sup>11</sup>



Pfeiffer *et al.*<sup>19</sup> achieved integration of oxygen and pH sensitive fluorescent dyes in a mask-less photo-polymerization process.

Sensor spots and foils are commercially available for dissolved oxygen in the range of 0–100% air saturation as well as for the detection of trace levels,<sup>20,21</sup> for pH in the range of pH 5.5–8 (ref. 21 and 22) and for carbon dioxide in the range of 1–25% CO<sub>2</sub> at atmospheric pressure.<sup>21</sup> Commercial sensor spots are typically available in diameters from 3 to 8 mm. This size is often impractical if the sensors need to be integrated into a small channel. Implementing a chamber of this size or larger to accommodate such a sensor spot can create dead zones and undesired flow patterns, and trap air bubbles. The smaller the sensor spot, the less challenging the integration. Indeed for microbio-reactors which have comparatively large chambers, these sensor sizes may not be critical for integration.<sup>5,23,24</sup> Spots can be glued into the channel, and sometimes silicone grease suffices. For microfluidic cell culture devices, certain (adherent) cell types have been observed to overgrow the sensor spots, which negatively affects the accuracy of the measurement.<sup>24,25</sup> Research into cell-repelling coatings and polymers is being conducted, but universal solutions to this problem have yet to be found and published.

### c. Sensor beads or particles

To avoid thermo-mechanical stress from heat-assisted bonding or sensor degradation due to solvents in adhesive-based bonding methods, it is best to introduce the sensors once the microfluidic device is fully assembled. This can for example be achieved using sensor nano- and microbeads or particles, which can be flowed *via* the fluidic ports to the detection area. This allows the use of thermally unstable sensor materials. The use of particles can yield in a higher signal for a better readout because the polymeric material can accommodate a higher dye concentration without inducing self-quenching effects (Fig. 2, d). Nanoparticles or micro- and nanobeads can be introduced into the system after it has been assembled and/or sterilized, provided the beads/particles are sterilized before their introduction into the system as well, if a sterile environment is necessary. Particles need to form stable dispersions in sample or culture media, and must not exhibit any interaction with cells. Micro-size particles are commercially available for oxygen detection.<sup>20,26</sup> To achieve a sufficiently strong read-out signal, a larger number of particles need to be held in place. Optical tweezers<sup>27</sup> or pillar-like structures within the channel have been used to trap the beads and keep them from being washed out by the fluid flow. As a further advantage of this approach, particles can be recovered after use.

Magnetic optical sensor particles (MOSePs), initially proposed by Mistlberger *et al.*, 2008,<sup>28</sup> held in place with a commercially available magnet, have shown promising results in terms of *in situ* sensor spot generation inside an already

bonded channel.<sup>29</sup> This enables the user to reposition the sensor particles and achieve flexible readout in the channel.

## 3. Deposition techniques for sensor layers

Stationary sensor layers minimise the risk of interference with sample, *i.e.* with cell metabolism and culture or luminescence quenching of dissolved substances as discussed in section 2.2. The fabrication method of the sensor layer, however, strongly influences signal strength, morphology of the resulting sensor layer, and stability of the sensor. Depending on the material with which the microfluidic device is fabricated, additional surface treatment may be required to support and to provide sufficient adhesion of the sensor material for flow-based applications. In this section, we discuss deposition techniques to create such sensing layers for microfluidic devices.

### a. Direct staining of device material

The material from which the device is fabricated, or parts thereof, can be directly doped with a sensing dye. This is relatively straightforward if, during device fabrication, the material is created by mixing together different components, such as in the case of the uncured poly(dimethylsiloxane) (PDMS) base and curing agents. Curing the PDMS with the mixed-in dye transforms part of the microfluidic device itself into a sensor. Challenges to consider for this method are the readout and the permeability of the polymer which functions as the sensor matrix. This method has found use in oxygen<sup>30</sup> and temperature<sup>31–33</sup> sensing. For these applications, dyed membranes were inserted in the reactor, meaning only parts of the reactor were doped.

### b. Spin- and knife-coating

Spin coating is an established technique in many industrial processes, *e.g.* semiconductors. Spin coating can produce homogenous layers on flat surfaces over a large area with a layer thickness down to a few hundred nanometres for optical sensor polymers.<sup>34,35</sup> The sensor formulation is applied to a smooth surface and spun in order to spread the fluid evenly using rotational force. Grist *et al.*<sup>36</sup> used this technique to create a sensor film which they then structured using laser ablation (see Fig. 3, B). A potential disadvantage of this method is that a lot of material is wasted during the spin-coating process. For knife coating, a matrix containing the sensor dye is first dissolved in a solvent, and then spread onto the surface using a 'knife'. The knife is positioned such that it produces a well-defined and small gap between the surface and the knife, thereby creating an even film. Polymer foils and glass slides are common carriers for knife coated sensors. This method is simple, but like spin coating, it requires a structuring post-process to obtain the desired sensor dimensions. For example, spots of a certain size are usually



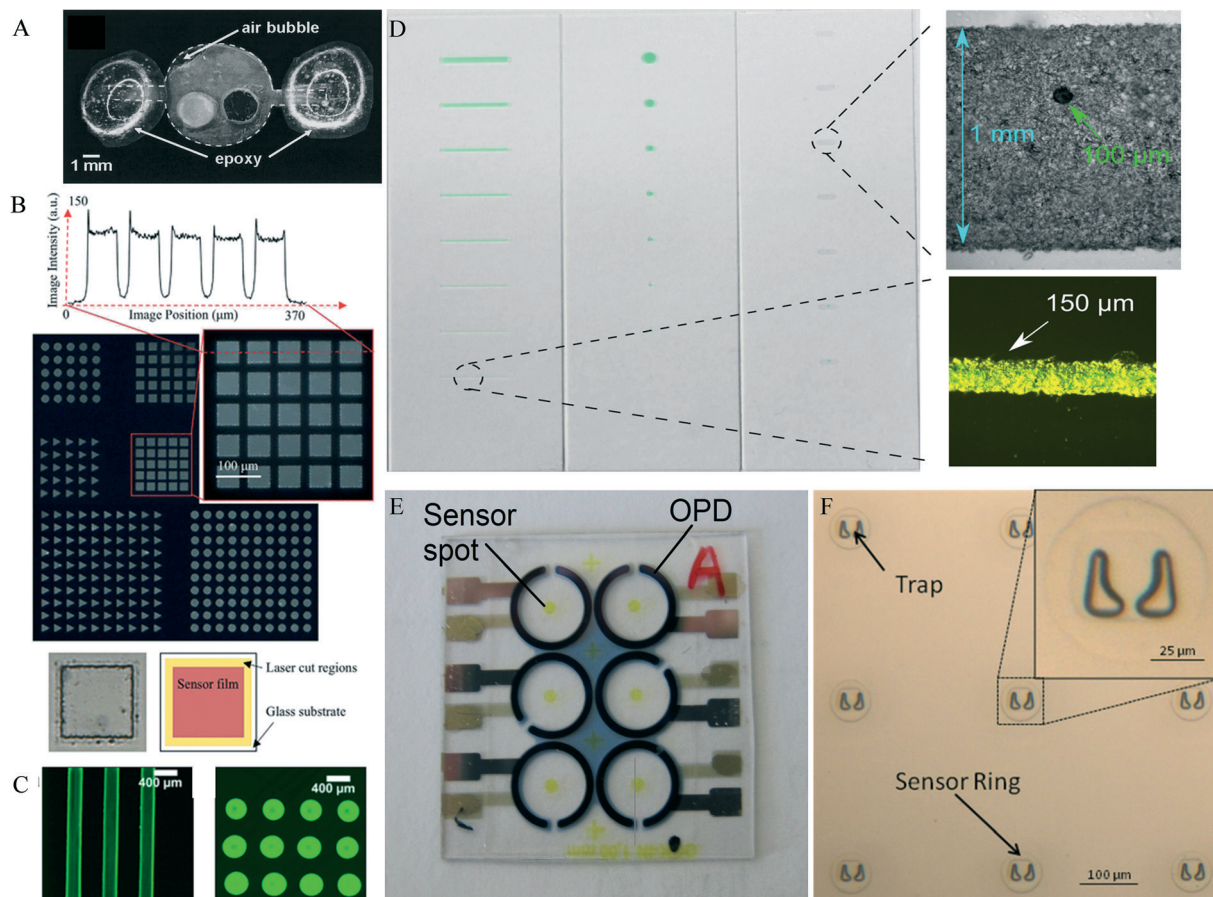


**Fig. 3** A – Commercially available optical oxygen sensor spot in microbioreactor (MBR) used for fermentation. Reproduced from ref. 23 with permission from John Wiley and Sons. B – (Top) Phosphorescence intensity images of patterned sensor films, showing arrays of 50  $\mu\text{m}$  squares, circles, and triangles on a pitch of 75  $\mu\text{m}$  (except the lower array of squares and inset, on a pitch of 65  $\mu\text{m}$ ). An intensity cross-section of the array of squares is also presented. The peaks at pattern edges are likely due to redeposition during the laser ablation. (Bottom) Bright-field image of one of the squares in the patterned array, as well as a diagram indicating the different regions (sensor film, laser ablation line showing the residue remaining after laser cutting, and glass substrate) within it. Reproduced from ref. 36 with permission from the Royal Society of Chemistry. C – Representative false-colored fluorescence images of inkjet-printed pH sensor microstructures in Britton–Robinson buffers (BRB) pH 10 with blue light excitation: (left) pH sensor rows and (right) pH sensor array (probes covalently bound to poly-hydroxyethyl-methacrylate (pHEMA) on glass) reproduced from ref. 45 with permission from the American Chemical Society. D – Sensing lines or spots ranging from 1000  $\mu\text{m}$  to 100  $\mu\text{m}$  in width or diameter and microscopic bright-field images of a 100  $\mu\text{m}$  sensor spot integrated into a 1 mm wide sensing area and of a 150  $\mu\text{m}$  wide sensor line. Lines and spots were prepared by airbrush spraying in combination with stencils. Microscopic bright-field images were taken with a monochromatic camera (spot) or a color camera (line) reproduced from ref. 43 under the terms of the Creative Commons Attribution License. E – Pictures of a polymer substrate with six organic photodiodes (OPDs) and screen-printed fluorescence sensor spots reproduced from ref. 38 with permission from SPIE. F – Microfabrication results showing an optical microscope image of a  $3 \times 3$  array of single-cell self-assembly traps encircled by an oxygen sensor embedded in SU8 rings with an insert of a magnified image of a trap and sensor ring reproduced from ref. 46 with permission from IOP Publishing.

cut out of the knife-coated foil and glued to a layer of the microfluidic device.<sup>34</sup>

### c. Screen-printing

In screen printing, the sensor cocktail (the matrix with the dye) is applied to the device through a specially prepared mesh which defines the size and shape of the sensor. The mesh is coated with a blocking stencil that is impermeable for the sensor cocktail. A squeegee blade then forces the cocktail through the apertures of the mesh and onto the device layer. This method is often used for applying electro-

chemical sensors onto their carrier substrate. With appropriate mesh and ink composition, feature sizes as small as 100  $\mu\text{m}$  can be achieved.<sup>37</sup> The disadvantage is that a lot of sensor material is wasted during the screen-printing, which can be a limitation for an expensive sensor matrix. Also, the deposition technique requires a planar surface, making the method unsuitable for application inside grooves. Thus microfluidic channels need to be formed in a separate layer, and then aligned and bonded to the screen-printed surface. This deposition technique has been demonstrated for optical sensors for oxygen, pH, and carbon dioxide by Mayr *et al.* (2012)<sup>38</sup> (Fig. 3, E).



#### d. Photo-polymerization

This method is useful for producing very small sensors with high dimensional accuracy. A photomask exposes only the desired area of a sensing dye-containing photoresist matrix with UV light. The photoresist matrix, such as poly(ethylene) glycol (PEG) hardens during the curing process creating the stationary sensor spot.<sup>39,40</sup> Alternatively, moulds with the desired sensor dimensions can be fabricated in polymers such as PDMS, which are then filled with the dye-doped photoresist. The mould polymer is removed after curing, leaving only the photoresist behind. Zhu *et al.* demonstrated a sensor patterning method which used photolithography to produce sensor layers in arbitrary shapes and sizes with high precision.<sup>35</sup> Related to photopolymerization, Nock *et al.*<sup>41</sup> demonstrated the use of photoresists for the production of a PDMS stamp for the integration of sensor layers. This method could also be referred to as micro contact-printing. Etzkorn *et al.*<sup>42</sup> used this method to create sensor rings wherein epithelial cells were trapped and their oxygen consumption monitored (see Fig. 3, F).

#### e. Spray-coating

In spray coating, the sensor cocktail (dyes and matrix polymer) are dissolved in a solvent that is suitable for the spraying process and also compatible with the device material. The technique enables homogenous coating of larger areas as well as the patterning of small areas through a stencil or mask. The smallest area reported for this technique is 2 mm × 2 mm (ref. 43) (Fig. 3, D). Layers can be structured down to a size of 100 micrometres combination with stencils.<sup>43,44</sup>

#### f. Microdispensing and inkjet printing

Best known for their use in the printing industry, microdispensing or inkjet systems deposit droplets of an ink by thermal, piezoelectric, acoustic, electrostatic, electrohydrodynamic actuation, or by using valves.<sup>47</sup> Microdispensing, in which a piezo-electrically guided tappet propels a droplet from a reservoir through a nozzle, is well suited for viscous sensing matrices or sensor material containing particles. Recently, this method has found application for the integration of pH sensors.<sup>17,45,48</sup> Other methods of droplet generation may be equally suitable for sensor integration and have in fact been used for the production of biosensors.<sup>47</sup> The thickness of the sensor layer can be varied by repeated dispensing onto the same area, or by adjusting the viscosity of the sensor matrix. Small dispensing nozzles are used to achieve a very fine deposition that can either be a continuous stream of droplets or discrete droplets. These techniques are well suited for printing sensors directly into microfluidic channels.

## 4. Sensor integration and microfluidic device sealing

Choosing the most suitable sensor deposition technique depends significantly on the material with which the microfluidic device was fabricated and how the device will be bonded and sealed. Exposure to elevated temperatures, organic solvents and even prolonged light exposure, particularly UV light, can all affect the sensor dyes and matrices, and they need to be considered when assembling the device. In the following section, we briefly discuss different device sealing and bonding methods and their potential impact on sensor performance.

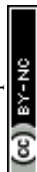
#### a. Clamping

When clamping devices, the layers of the microfluidic device are connected only by the mechanical pressure exerted by the clamping structure.<sup>49–52</sup> Whilst achieving a leak-free system can be challenging, usually requiring a clamping system customized to the device design, the obvious benefit is that access to the channels and structures inside the microfluidic device is possible at any time.<sup>49</sup> This facilitates not only the deposition, but also subsequent addition or replacement of sensors. Clamping systems are also commercially available.<sup>53,54</sup>

#### b. Heat-assisted bonding methods

Thermo-compression bonding is a direct bonding method, which is typically suited to bond identical polymer or glass substrates<sup>55</sup> and which creates irreversible bonds. The substrates are mechanically pressed together and heated to a high enough temperature (above the glass transition temperature for polymers) to effect the bonding. Sensor dyes and matrices, however, typically operate within a confined temperature range, and are prone to degradation at most bonding temperatures. Some commercially available oxygen sensor dyes are capable of withstanding temperatures suitable for bonding PMMA and autoclavation (120 degrees Celsius),<sup>20,21</sup> although their sensitivity might change through the process and re-calibration might be necessary after bonding or sterilization. Temperature stability has also been shown for sensors of other analyte; Gruber *et al.*<sup>17</sup> bonded a PMMA reactor at 110 °C for over 45 minutes with pH sensors integrated in the reactor. After thermal bonding the sensors still showed excellent pH sensitivity.

Anodic bonding, also referred to as field-assisted bonding, is usually used to bond glass to silicon. During this method, the glass, which has to be a borosilicate glass with a high content of alkali ions, is exposed to an electric field, causing the surface of the glass to bond with the surface of the silicon wafer. This usually happens at high temperatures >300 °C, but has been shown to work at temperatures as low as 180 °C by Ehgartner *et al.*<sup>43</sup> which is more likely to leave sensing material in a functional state. With the current state of the art in sensor dye and matrix development, anodic bonding will



have to be effective at even lower temperatures to allow sensor integration.

### c. Plasma bonding

In plasma-assisted bonding methods, the cold plasma activates the surface of the substrate, which can create an irreversible bond when two substrates are brought into intimate contact with each other. This allows the bonding of two substrates of different materials at low temperatures, such as PDMS to glass.<sup>56</sup> Though a low temperature process, the plasma itself can affect the sensor composition. Nock *et al.*<sup>41</sup> used plasma bonding to integrate a sensor dye stained PDMS layer into their reactor, in this case the plasma was used on the reactor material to make the PDMS sensor material stick to the bottom of the reactor. Lee *et al.* used PDMS curing both for the production of their sensors as well as for sealing the channels with a glass lid.<sup>13</sup>

### d. Adhesive bonding

In adhesive bonding, an intermediate layer is applied between the two to-be bonded materials; this can be a photoresist, a sputtered glass or different polymers.<sup>55</sup> Often, UV-curable glue is used to connect microfluidic device layers to each other. Glue has the advantage of being liquid and easy to handle, and to harden when exposed to UV light, thereby bonding the substrates.<sup>57</sup> For many sensor dyes the constant excitation caused by prolonged exposure to UV light can lead to bleaching.

### e. Solvent-assisted bonding

For devices fabricated out of thermoplastic polymers, low temperature bonding can be achieved by softening the polymer surfaces with an organic solvent prior to thermo-compression bonding. This can reduce the bonding temperature well below the glass transition temperature and is often used for bonding microfluidic devices. In the future this technique could be developed into a method favourable for sensors with low heat resistance. However, to date, examples of solvent-assisted bonded devices with optical sensors have not been reported. A possible drawback of this method is that solvent fumes can get to the sensor material and affect their integrity. Minor splashes or fumes also soften or reflux polymers which can deform and clog channels.<sup>58</sup>

## 5. Luminescence detection principles

Optical sensors have gained popularity for monitoring since they allow online and non-destructive measurements in microfluidic devices. Also, in most cases, the cut-off wavelengths of the polymers are beyond the wavelength ranges of the sensor. Many of these sensors are based on photoluminescence or absorption. Photoluminescence is a term encompassing phenomena of fluorescence, phosphorescence and delayed fluorescence. Optical sensors based on photoluminescence are typically selective to the analyte and highly

sensitive, since emission spectra are specific to the dyes used in the sensor, making interference with the reagents and samples in the microfluidic device unlikely.<sup>59</sup> Depending on the measurement principle and sensor format, various read-out methods can be considered. Among them are fluorescence microscopy, optical fibers, and integrated read-out techniques consisting of a light source and a detector in close vicinity to the sensor. For these, the detectors can be on the same side as the light source or opposite. A further method is the determination of absorption using a spectrophotometer. The most common readout principles will be briefly introduced in this section; Fig. 4 can be consulted as a visual aid in understanding the principles.

### a. Detection of intensity

Detection of luminescence intensity is straightforward since it requires simple instrumentation. Standard fluorescence microscopy set-ups can for example be used. However, luminescence intensity measurements are sensitive to variations in the illumination pathway, including the light source itself, interfering ambient light, and variations in the detectors. The quantification of the analyte can also be affected by variation of the concentration of the dyes in the matrix, photo-bleaching, and light scattering. Therefore, lifetime measurement and ratiometric methods are typically preferred.

### b. Single-photon counting

Single photon counting or time-correlated single photon counting (TCSPC) determines the lifetime of an excited state in the time domain. Individual photons are counted using a photodetector after excitation of the dye with a short laser pulse. The time measured between the excitation and the detected photon is stored in a histogram representing the decay curve. The lifetime is obtained by an exponential fitting function (Fig. 4, a). The method enables accurate measurements for short decays in the nanoseconds range. This would be suitable for measurements with pH-indicator dyes but requires expensive and complex instrumentation. Online monitoring with this technique is also limited by a relatively long acquisition time. So far this principle has been shown by Bennet *et al.*<sup>60</sup> who used it for temperature measurement in a microfluidic microscopic imaging setup.

### c. Time-gated fluorescence

This is another method where the lifetime is determined in the time domain. Again, a luminophore is excited by a pulse, after which the emission phase is recorded in two or more successive 'time-gates', meaning the luminescence decay is monitored in set time intervals. The images obtained during these time-gated periods are used to determine the luminescence lifetime *via* the ratio of the intensities measured in the time gates.<sup>61</sup> A variety frequently employed for lifetime imaging is 'rapid lifetime







Fig. 4 Schematic representation of measurement methods applied *via* optical sensing (intensity measurements not shown). (a) Luminescence lifetime determination by time-correlated single photon counting (TCSPC). (b) Lifetime determination by gated detection: rapid lifetime determination shown. (c) Lifetime determination by phase modulation. (d) Dual wavelength ratioing. Reproduced from ref. 66 with permission from Elsevier.

determination' where the sample is excited and the luminescence intensity is recorded in two time gates<sup>29,62,63</sup> (Fig. 4, b). Ruthenium tris-2,2-dipyridyl dichloride hexahydrate (RTDP) has been used as an oxygen sensitive dye for fluorescence life-time based imaging in a PDMS chip for cell culturing.<sup>14,64</sup>

#### d. Phase modulation

In this method, the lifetime is determined in the frequency domain. The luminophores are excited with an amplitude-modulated light source, for example a sinusoidally modulated light. The resulting emission follows the modulation with a certain time delay, which depends on the lifetime of the luminophore. This delay can be measured as a phase shift by a lock-in amplifier and used to calculate the lifetime (Fig. 4, c).<sup>23,43</sup> Instrumentation is inexpensive for lifetimes >1  $\mu$ s and is miniaturized to the size of a memory stick as used by Ehgartner *et al.*<sup>43</sup> Phase shift measurements show lit-

tle cross-sensitivity to ambient light and are applied for single point oxygen measurements in microfluidic devices.<sup>23,43</sup>

Dual lifetime referencing DLR enables referenced signals for analyte-sensitive fluorophores with decay times in the nanosecond range (most pH-indicators) with fiber optic instrumentation. A reference dye with overlapping absorption spectra and lifetime in the micro-second range is added to the sensor layer.<sup>65</sup> This method is frequently used for pH sensing.<sup>17,23,48</sup>

#### e. Two wavelength ratioing

This method relies on two bands in the emission spectra detected at one emission wavelength. An inert reference dye is added, if the sensor dyes do not show two bands in the emission spectra that can be separated. The ratio of the two emission signals is related to the analyte concentration. The challenge for miniaturisation is to achieve sufficient signal from emission bands as well as implementing a suitable



readout setup. Color CCD cameras have been shown to be suitable for this task.<sup>34</sup>

## 6. Measurement systems and applications

To showcase the broad applicability of the sensors, this section discusses successful systems that have been presented over the past few years with a focus on particular analytes, namely oxygen, pH, carbon dioxide, glucose, and temperature. Another vital process variable is the optical density (OD). The OD can be determined *via* absorption<sup>67</sup> measurements, but does not require the integration of a sensing material and will therefore not be discussed here. Multiparametric sensor configurations are discussed at the end in a separate sub-section.

### a. Oxygen

Optical oxygen monitoring is by far the most successfully implemented analytical parameter of online monitoring in microfluidic systems; firstly, because oxygen is one of the most important parameters in applications ranging from cell culture monitoring to fermentation or biocatalysis and, secondly, because of its simple sensing principle. In addition, optical oxygen sensing has become an established technique in process monitoring. Complete detection systems, including read-out boxes, probes, patches and micro sensors are commercially available and can be used in microfluidic devices and microreactors.<sup>20,21</sup>

Optical oxygen sensors are comprised of a phosphorescent indicator dye immobilised in a lipophilic host polymer. The sensing principle is based on the quenching of the phosphorescence of the dye by molecular oxygen. The decrease of the luminescence intensity ( $I$ ) in lifetime ( $\tau$ ) is a result of energy transfer from the energetically excited dye to the oxygen, which is transferred into its excited singlet state ( $S_1$ ), while

the excited oxygen indicator returns to its ground state ( $T_1$ ) by radiation-free deactivation. The generation of singlet oxygen can be critical in small scales since it can lead to oxidation of sensor matrix components which can lead to oxygen consumption and affect the oxygen concentration in the microchannel.<sup>29</sup> The sensitivity of the oxygen sensor is influenced by the phosphorescence lifetime of the indicator and the oxygen permeability of the host polymer. This enables a tuning of the sensitivity of the oxygen sensor, *e.g.* anoxic conditions or ambient dissolved oxygen concentration. It is especially important to choose a sensor matrix that does not store the analyte in question *i.e.* oxygen or carbon dioxide for trace oxygen sensors. The most commonly used dyes and host polymers are summarized in Table 2. In most cases, the oxygen concentration is monitored *via* the decay of phosphorescence intensity or lifetime. A typical plot of the lifetime *vs.* oxygen partial pressure is shown in Fig. 4b. A linearization method for the oxygen quenching is the Stern–Volmer plot, in which the oxygen content of a system is plotted against the luminescence intensity,  $I$ , over the luminescence intensity in the absence of oxygen,  $I_0$ , or the luminescence decay time,  $\tau$ , over the luminescence decay time in the absence of oxygen,  $\tau_0$ :

$$\frac{\tau_0}{\tau} = \frac{I_0}{I} = 1 + K_{SV}[Q] \quad (1)$$

where  $K_{SV}$  is the Stern–Volmer constant which consists of the molecular quenching rate constant multiplied by the excited state lifetime in the absence of the quencher  $Q$ . It is important to be aware of the fact that these parameters change under the influence of temperature and that the optical oxygen sensor measures partial pressure. Oxygen concentration is then obtained by Henry's law.

Oxygen sensors are of particular interest in oxygen-dependent processes, such as fermentations, whole cell syntheses or stem cell culture. Most oxygen sensors are suitable

**Table 2** Advantages and disadvantages of the three most commonly employed sensor formats in regards to integration and practical application

| Sensor format           | Advantages   | Disadvantages   |
|-------------------------|--|---|
| Dissolved indicator dye | <ul style="list-style-type: none"> <li>- Easy to implement for simple measurements</li> <li>- Spatial analyte imaging possible (but requires a suitable detection system)</li> <li>- Universally applicable, largely independent of chip design</li> <li>- Application after device bonding</li> <li>- Readout anywhere in device</li> </ul> | <ul style="list-style-type: none"> <li>- Indicators have to be added and removed from sample</li> <li>- Homogeneous dispersion of dye required for accurate readout</li> <li>- High concentrations necessary for signal strength</li> <li>- Potential interference with sample</li> </ul> |
| Layers or spots         | <ul style="list-style-type: none"> <li>- Stationary</li> <li>- Easy to use once integrated</li> <li>- No separation steps necessary</li> <li>- Interference with sample unlikely</li> </ul>  | <ul style="list-style-type: none"> <li>- Can be difficult to integrate</li> </ul>   |
| Beads or particles      | <ul style="list-style-type: none"> <li>- Ease of use once developed</li> <li>- Application after device bonding</li> <li>- Flexibility in chip design and production</li> <li>- Readout anywhere in device</li> <li>- Less interference with sample compared to dissolved indicators</li> </ul>  | <ul style="list-style-type: none"> <li>- Particles have to be added and removed from sample</li> <li>- Homogeneous dispersion of particles required for accurate readout</li> <li>- Poor stability of the suspension of particles can lead to inhomogeneity</li> </ul>                    |





Table 3 Sensor materials, dyes and format used for oxygen, pH and carbon dioxide monitoring sorted by analyte

| Analyte  | Dye  | Sensor matrix                                    | Range                           | Integration method  | Bonding method   | Readout   | Application                                 | Reference           |
|--|--|--|---------------------------------|---------------------|------------------|---|---|---------------------|
| O <sub>2</sub>   | Platinum porphyrin (platinum(II)-5, 10, 15, 20- <i>meso</i> -tetraphenyltetra <i>benzoporphyrin</i> )              | Polystyrene (PS) nano-particles                  | 0–100% air saturation           | In flow             | —                | Flow-through fluorimeter and photometer                           | Cell culture                                | 71                  |
|  | Ruthenium tris(2,2'-dipyridyl) dichloride hexahydrate (RTDP)   | —  | 0–100% air saturation           | Dissolved indicator | —                | Fluorescence lifetime-based imaging                               | Cell culture                                | 14                  |
|  | Platinum(II) octaethylporphyrin ketone (PtOEPK)  | PS   | 0–100% air saturation           | PDMS stamps         | Plasma bonding   | Fluorescence intensity imaging                                    | System development                          | 41                  |
|  | Pt(II) <i>meso</i> -tetra(pentafluorophenyl)porphine (PtTFPP)  | Poly styrene maleic anhydride (PSMA)             | 0–100% air saturation           | Magnetic forces     | —                | Fiber optics/imaging  | Proof of concept                            | 29                  |
|  | Pt(II) <i>meso</i> -tetra(pentafluorophenyl)porphine (PtTFPP)  | SU8  | 0–100% air saturation           | Photo-patterning    | Chemical         | Lifetime measurement  | Proof of concept                            | 29                  |
|  | Palladium(II) - or platinum(II) <i>meso</i> -tetra(4 fluorophenyl)tetra- <i>benzoporphyrin</i> (PtTTPBPf/ PtTFBPf) | PS/silicone composite material                   | 0–25%, 0–100% air saturation    | Spray coating       | Heat/anodic      | Microscopic imaging   | Single cell monitoring                      | 46                  |
|  | Platinum(II) <i>meso</i> -tetra(4 fluoro-phenyl)tetra <i>benzoporphyrin</i>  | PS-PVP nanoparticles                             | 0–100% air saturation           | In flow             | —                | Luminescent lifetime measurements with fiber optics               | Enzymatic reactions                         | 43                  |
|  | Fluorescein-5-isothiocyanate ( <i>p</i> -HEMA)   | Poly-hydroxyethyl-methacrylate ( <i>p</i> -HEMA) | pH 5.5–pH 10.5                  | Ink-jet printing    | Chemical         | Luminescent lifetime measurements with fiber optics               | Microorganism                               | 73                  |
|  | Seminaphtho-rhodafuor derivative (SNARF)   | Functionalized surface                           | pH 6.2–pH 6.9                   | In flow             | —                | Fluorescence intensity imaging free-flow isoelectric focusing     | pH gradient monitoring and pH determination | 45                  |
|  | Aza-BODIPY dye array   | PS-beads   | pH 7.4–11.5                     | Microdispensing     | Thermal          | CCD imaging and two wavelength ratioing                           | System development                          | 16, 27              |
|  | Aza-BODIPY dye   | Hydrogel D4                                      | pH 3.5–7.5, pH 5–9, pH 6–pH 8.5 | Microdispensing     | Thermal          | Dual lifetime referencing with fiber optics                       | Proof of concept                            | 17, 48              |
|  | pH   | Vinylsulphonyl azo-dye                           | PS-PVP nanoparticles            | pH 5.5–pH 8.5       | In flow          | —   | Dual lifetime referencing with fiber optics | Enzymatic reactions |
| 8-Hydroxypyrene-1,3,6-trisulfonate (HPTS)  |  | TentaGel macrobeads                              | pH 7–10.5                       | In flow             | —                | Dual lifetime referencing with fiber optics                       | Enzymatic reactions                         | 7                   |
| Phenol red   |  | Poly-hydroxyethyl-methacrylate ( <i>p</i> -HEMA) | pH 6.5–10                       | In flow             | —                | Micro spectrophotometry   | System development                          | 76                  |
| 6-Carboxynaphthofluorescein (CNF) and ruthenium-tris-(1,10-phenanthroline) <sup>2+</sup> |  | Poly(ethylene glycol) diacrylate (PEG-DA)        | pH 5.8–8.2                      | Photo-patterning    | Plasma bonding   | Micro flow-through fluorimeter                                    | Proof of concept                            | 77                  |
| Bromothymol blue   |  | Poly-hydroxyethyl-methacrylate ( <i>p</i> -HEMA) | pH 6.5–pH 9                     | Spin-coating        | —                | CCD imaging with diodes, coupling optics and interference filters | Cell culture                                | 13                  |
| Fluorescein  |  | —  | 0.26–10 g L <sup>-1</sup>       | Dissolved indicator | Lamination       | Fluorescence lifetime-based imaging                               | Cell culture                                | 78                  |
| Cresol red, pyranine   |  | Dowex® chloride form                             | —                               | Dissolved indicator | —                | Micro spectrophotometry   | Wine and beer                               | 15                  |
|  |  | —  | —                               | Dissolved indicator | Solvent assisted | Fluorescence quenching imaging                                    | Environmental                               | 79                  |
|  |  | —  | —                               | Sensor layer        | —                | Micro spectrophotometry   | System development                          | 80                  |
|  |  | —  | —                               | —                   | —                | —   | Proof of concept                            | —                   |

for autoclaving and therefore reusable, which means that microfluidic devices can also be re-used as long the material they are made of is autoclavable too (Table 3).

A comprehensive review by Wang *et al.*<sup>4</sup> further summarised optical methods for sensing and imaging oxygen, focusing on materials, spectroscopic methods, and applications at a larger scale. Many papers have described the use of oxygen sensors in lab-on-a-chip or lab-on-a-disk technology, showing a variety of different dyes and polymeric matrices being used for this purpose. In 2013, Jin *et al.*<sup>68</sup> presented a platinum porphyrin-based, NIR luminescent copolymer for the measurement of dissolved oxygen in microreactors, these were covalently bonded to the polymer. Sensor materials, with absorption/emission profiles in the red or near-infrared, are beneficial because this will reduce scattering and background signal due to the low absorption and auto-fluorescence of biomolecules in the NIR spectral region.

Oxygen sensors have also been applied to the monitoring of stem cells in a microfluidic cell culture device. Super *et al.*<sup>24</sup> used commercially available sensors to quantify in real time and non-invasively the specific oxygen uptake rates of CHO and embryonic stem cells over several days of culture. Grist *et al.*<sup>69</sup> designed a microfluidic reactor suitable for the control of oxygen levels in a chamber with the intent of using the reactor as a tool to study hypoxia in cells. A platinum porphyrin dye in polystyrene was spin coated onto a glass slide. The desired shape of the channel was cut out of the spin coated layer using laser ablation; the resulting sensor patch was then integrated into the microfluidic device. Ehgartner *et al.*<sup>43</sup> showed the possibility of a time-course profile for oxygen sensors along the meandering channel of a microfluidic device by monitoring multiple sensor spots simultaneously (see Fig. 5) and (6).

A microfluidic perfused 3D human liver model was introduced by Rennert *et al.*<sup>44</sup> This functional liver organoid was

comprised of all major liver cell types. With the aid of spray-coated optical oxygen sensors spots it was possible to measure the respiration of the organoid. The device and sensors can be seen in Fig. 7.

Molter *et al.*<sup>64</sup> demonstrated the capability of monitoring a single cell in a microarray using fixed luminescent oxygen sensors at the side of the microarray wall. Etzkorn *et al.*<sup>46</sup> showed the use of SU8, a photo-patternable resin, as a sensor matrix and also for the use of trapping single cells for this monitoring of their oxygen consumption rate. Oomen *et al.*<sup>70</sup> published a tutorial review for the implementation of oxygen control in microfluidic cell and tissue cultures that discusses the challenges for these applications in great detail.

2D oxygen imaging has been used frequently<sup>41,46,64</sup> and is an established method nowadays, whereas the imaging of other analytes is still a challenge. For the process the microscope is used to measure the light intensity emitted by the dye. The sensor can be photopatterned,<sup>41</sup> spray-coated, or knife-coated.<sup>34</sup> A reference signal is necessary in order to achieve reliable imaging, since the distribution of light and dye cannot be considered to be homogeneous.

Ungerböck *et al.* have shown the possibility of low cost operation using RGB cameras<sup>34</sup> to measure a knife-coated sensing film. A review by Sun *et al.* (2015)<sup>11</sup> summarizes the advances in oxygen imaging development for microfluidic devices very nicely and could be consulted for further details on oxygen imaging. Nanoparticles and dissolved indicator dye are particularly useful for monitoring parameters in aqueous droplets suspended in an organic phase, since sensor layers cannot be applied in a system like that. Cao *et al.*<sup>71</sup> demonstrated the use of oxygen-sensitive nanoparticles for the monitoring of bacterial growth in a microfluidic droplet-based system capturing oxygen changes during metabolic activity. Bavli *et al.*<sup>72</sup> have shown the advantages of oxygen microbead sensors in a liver-on-a-chip system where they were used to measure oxygen uptake under static conditions.

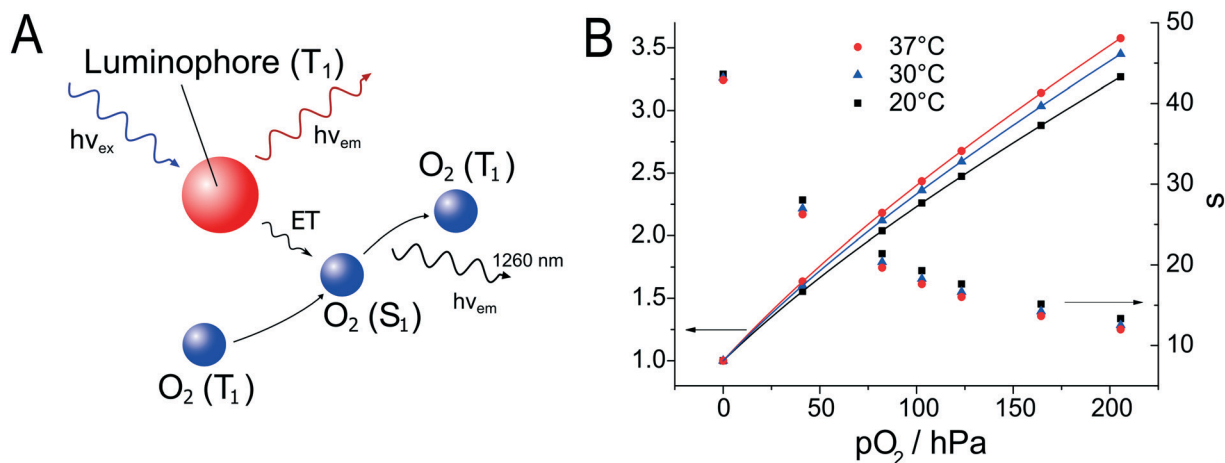
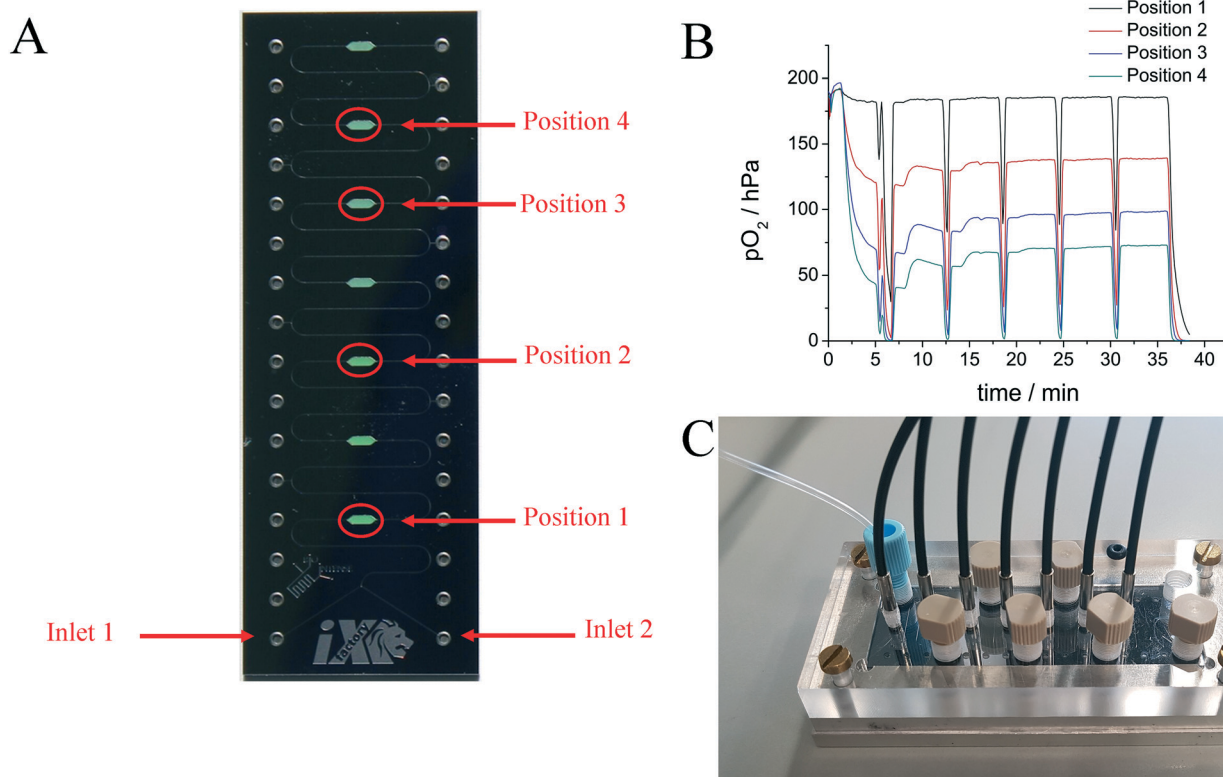
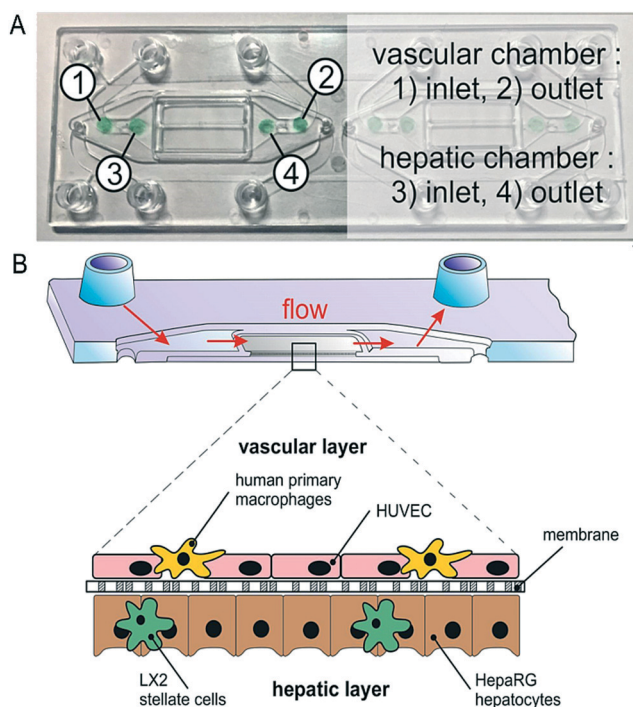


Fig. 5 A – Schematic depiction of the oxygen sensor scheme. Luminophore is excited and emits (red arrow) from the triplet state ( $T_1$ ). The emission is quenched by a collision with molecular oxygen, which is transferred to the singlet state ( $S_1$ ) and deactivated by the emission of IR radiation (black).<sup>106</sup> B – Stern-Volmer calibration curves (left Y-axis) and luminescent lifetimes (right Y-axis) for integrated oxygen sensor layers in at 20 °C, 30 °C, and 37 °C reproduced from ref. 43 under the terms of the Creative Commons Attribution License.





**Fig. 6** A – Sensor chambers fully covered by oxygen sensors in microreactor, the monitored chambers are indicated *via* red circles. B – Oxidation of D-alanine by D-amino acid oxidase at a flow rate of  $0.6 \mu\text{L s}^{-1}$ , monitored in the four positions. C – MBR in holder with optical fibers attached to read-out the integrated sensors. Reproduced from ref. 43 under the terms of the Creative Commons Attribution License.



**Fig. 7** Integration of oxygen sensor spots in the microfluidically supported biochip. Sensor spots were integrated at the inlets (1, 3) and the outlets (2, 4) of the upper and lower channel systems, respectively. Reproduced from ref. 44 with permission from Elsevier.

Thomas *et al.* (2009)<sup>25</sup> were able to use a thin film sensor for oxygen imaging for *in vitro* mammalian cell culture for over 60 hours.

Recently, Horka *et al.*<sup>73</sup> showed that the lifetime of phosphorescent nanoparticles could be used accurately to determine the oxygen concentration in microdroplets to monitor the metabolism of bacterial cells. For this purpose, a phosphorescent indicator dye was embedded in poly(styrene-*block*-vinylpyrrolidone) nanobeads. The optical density was monitored at the same time to monitor the growth of the microorganism in the microdroplets.<sup>74</sup> Abbyad *et al.*<sup>75</sup> showed that they were able to control the oxygen levels in water droplets separated by a perfluorinated carrier oil from a partial pressure of 1 kPa to ambient partial pressure of 21 kPa. With fluorescence lifetime measurements of a ruthenium based dye, they could monitor the oxygen content in the droplet to verify the fast equilibrium between the inside of the droplets and the carrier oil. Red blood cells were used for the purpose of oxygen monitoring in this experiment.

Using the previously mentioned magnetic optical sensor particles (MOSePs), Ungerböck *et al.* (2014)<sup>29</sup> applied oxygen sensitive particles produced *via* nano-precipitation and Pt-benzoporphyrine or Ir-coumarine dyes to show that these particles can be moved along the channel *in situ*, thereby allowing the measurement of oxygen at any given position in the channel once they have been trapped with a magnet.



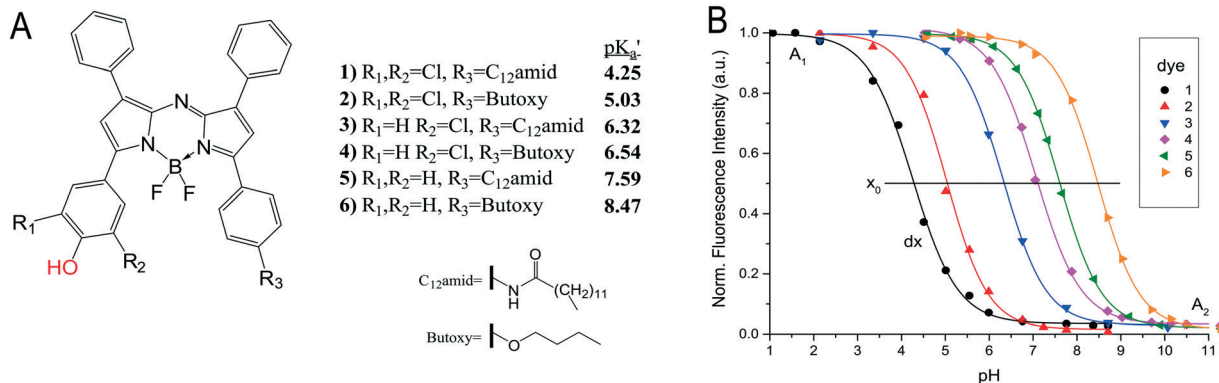


**Fig. 8** A) Chemical structures of NIR emitting aza-BODIPY dyes. The protonated/deprotonated group is marked in red. Synthetic modification  $R_1$ ,  $R_2$  and  $R_3$  are used to tune the  $pK_a$  value of the dyes. The lipophilic chain ( $R_3$ ) is used to immobilise the dye in hydrogel polymer. B) Calibration curves of dye 1–6, embedded in a hydrogel matrix from emission spectra. (Adapted from Strobl *et al.* 2015) reproduced from ref. 81 under the terms of the Creative Commons Attribution License.

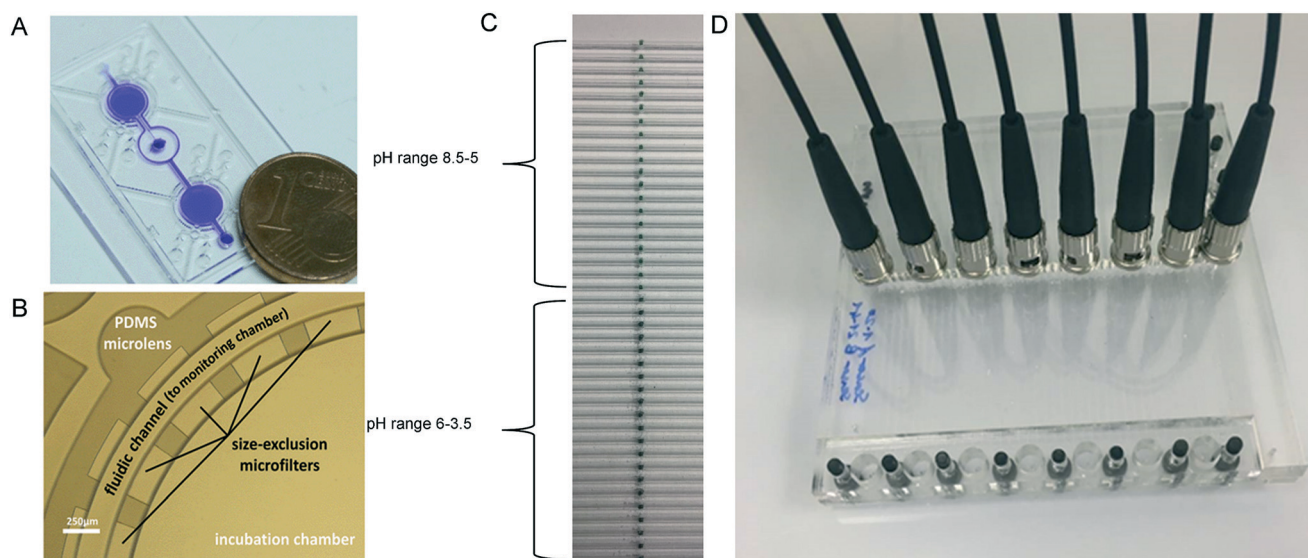


**Fig. 9** (A) Photograph of the microchip filled with crystal violet dye (for validation purposes). (B) Magnification of a section of the incubation chamber with PDMS microlenses for light coupling, fibers were held in place by openings in the housing of the device. Reproduced from ref. 85 with permission from the Royal Society of Chemistry. (C) Photograph of the sensor array in the microfluidic side entry reactor ( $\mu SER$ ) consisting of the sensor spots to detect pH between pH 8.5 and 5, and the sensor spots for a pH between 6 and 3.5 in the top and bottom half of the reactor, respectively. (D) Photograph of the  $\mu SER$  with the fibers for the pH sensor read-out held in the slots of the fiber holder plate. The slots corresponded to the sensor positions 1 to 8 shown in the schematic representation of a reproduced from ref. 17 under the terms of the Creative Commons Attribution License.

## b. pH

Monitoring pH is as important as oxygen for many biotechnological processes. It is essential to the activity of enzymes, the stability of substrates and products, as well as the chemical state of components in a reaction mixture. In optical sensor technology, the pH is typically monitored by measuring changes of the absorbance or fluorescence on protonation or deprotonation of an indicator dye (see Fig. 8A). For the use in sensor foils and layers the indicator is lipophilised and embedded or covalently linked to a hydrophilic polymer. The

acid base equilibrium of the indicator is typically limiting the operating range to 3 pH units. Although this is sufficient for most applications in biotechnology, a way to circumvent this drawback is by using multiple pH indicators that exhibit the same spectral properties but for different apparent  $pK_a$  values, as shown in Fig. 8. A mixture of these dyes immobilised in one sensor spot enabled sensors to cover the pH range from pH 2 to 9 though at the expense of a lower sensitivity.<sup>81</sup> Alternatively, each dye can be immobilised individually in several sensor spots to create an array of pH



sensors. The array then covers a broad pH-range whilst retaining the high sensitivity of individual optical pH sensors (Fig. 9).<sup>17,81</sup>

Typically, calibration curves can be described with a Boltzmann-fit. A multi-point calibration of three or more points is recommended for an accurate fit and to obtain good results, and follows the equation:

$$y = \frac{A_1 - A_2}{1 + e^{(x-x_0)/dx}} + A_2 \quad (2)$$

where  $A_2$  is the value for low fluorescence,  $A_1$  is the value for high fluorescence,  $x_0$  is the point of inflection ( $\text{pKa}'$ , apparent  $\text{pKa}$ ), and  $dx$  is the slope at the point of inflection. Table 2 summarizes pH sensitive dyes, which were implemented for the monitoring of pH in microfluidic systems. These include frequently used dyes 8-hydroxypyrene-1,3,6-trisulfonic acid (HPTS), carboxyfluorescein derivatives and seminaphthorhodafluors (SNARFs), which suffer from several drawbacks. Fluorescein derivatives and SNARFS have only moderate photostability, and the  $\text{pKa}$  value of HPTS is highly dependent on the ionic strength of the solution.<sup>82</sup> Recently, the Klimant group published optical pH sensors based on aza-BODIPY dyes (see Fig. 7) with remarkable photostability and low dependence on ionic strength.<sup>81,82</sup> Moreover this dye class is excitable with red light and emits in the NIR spectral regions, offering the advantages mentioned above. In addition to a suitable pH range, photostability, cross-sensitivity to ionic strength, excitation and emission wavelengths, the choice of a dye also depends on the host polymer. Covalently binding dyes, as well as physically entrapping them in a polymer matrix can lead to a shift in the pH range of the dye. It is important to note that hydrophilic matrix polymers do not withstand sterilisation procedures such as autoclaving.

The number of publications on pH with integrated pH measurements is smaller compared to oxygen. Jezierski *et al.*<sup>83</sup> introduced a fluorescent pH sensors system for online monitoring of a free-flow electrophoresis chip. The sensors were integrated to observe the pH gradient in the so-called microfluidic free-flow isoelectric focusing system in real time. This system allows for monitoring throughout the entire process without the addition of markers to the sample. Recently, Gruber *et al.*<sup>17</sup> presented a microfluidic side-entry reactor with an array of optical DLR-based sensors at several positions in the chip which allows for the continuous online monitoring of enzymatic reactions and their progression. Additionally, they were able to use the pH sensor feedback to counteract the pH drop caused by acidic products and keep the pH in the reactor within the operating parameters of the enzyme. The possibility of pH and dissolved oxygen measurement within cell culture media was shown by Lee *et al.*,<sup>13</sup> however this was what we might consider to be an at-line measurement, since some of the sensors weren't integrated directly in the microfluidic device but rather in a separate measurement cell.

Funfak *et al.*<sup>77</sup> successfully showed optical pH sensing with a flow-through fluorimeter using HPTS dye-doped polymer particles to monitor the pH during cell cultivation in a droplet-based flow system. Klauke *et al.*<sup>27</sup> used optical tweezers to maintain particles in position after they have been introduced into the system.

In their 2008 paper, Brigo *et al.*<sup>76</sup> presented 300–400  $\mu\text{m}$  TentaGel resin beads with immobilized covalently bound pH sensitive azo-dyes. These beads, which consist of polyethylene glycol attached to cross-linked polystyrene, were used in a PDMS on glass chip; the measurement of the pH was possible *via* a micro-photometer consisting of a confocal microscope, coupled to a diode-array spectrophotometer with an optical fibre. The beads have a response time of several minutes, due to the slow diffusion within the resin beads.

A high throughput optical sensor array was developed for the online monitoring of the pH of a cell culture by Wu *et al.* in which the light transmission efficiency through various thicknesses of PDMS layers was studied.<sup>84</sup> Dissolved indicators were also used by Muñoz-Berbel *et al.*<sup>85</sup> in a PDMS chip, featuring a monolithically integrated filter with size exclusion microchannels for the monitoring of a cell culture OD (at various wavelengths) and pH by measuring the absorption of phenol red in the system.

Del Ben *et al.*<sup>16</sup> used Snarf-5F as a dissolved pH indicator dye in compartmentalized single cell droplets on a microfluidic platform to detect circulating tumour cells (CTCs) through their metabolism, which causes the acidification of the media in the droplet and the secretion of lactate. Therefore two-wavelength ratioing of the Snarf-5F dye was utilized to determine the lactate concentration indirectly.

In section 6.f more systems that incorporate online pH monitoring are described, which also include the online monitoring of other parameters and are therefore highlighted.

### c. Carbon dioxide

Carbon dioxide is an important culture variable relevant for all adherent cell cultures, and relevant to understand fermentations or the progression of bio catalytic reactions.<sup>86</sup> So far, very few papers have reported successful systems for the monitoring of this analyte at a microscale. The optical  $\text{CO}_2$  sensors that are probably most suitable for miniaturisation function on the principle of a pH change within the sensor when the sensor is in contact with  $\text{CO}_2$ . This change in pH is detected *via* the use of an indicator dye. These sensors are often referred to as dry concept or solid state sensors as described by Mills, therefore also known as Mills' type sensors.<sup>87</sup>

A Mills' type sensor consists of a hydrophilic polymer matrix, usually a hydrogel, and a quaternary ammonium base (the most popular being tetraoctylammonium hydroxide), which forms an ion pair with the pH-sensitive indicator dye. The pH sensitive layer is covered a lipophilic protective layer to prevent interference from protons and other ionic species.



The sensors can only be used in humid or aqueous environments because water molecules are necessary for the pH sensitive dye to function as an indirect indicator for the CO<sub>2</sub> concentration through the following bicarbonate equilibrium equation:



where Q<sup>+</sup> and Ind are the quaternary ammonium ion and indicator dye, respectively.

In an adaptation of the Mills' type carbon dioxide sensor, Zilberman *et al.*<sup>80</sup> used cresol red and pyranine in combination with the quaternary ammonium ion, tetraoctylammonium hydroxide, to create a sensing matrix that was poured into sensing wells for the monitoring of carbon dioxide with ion exchange resin beads doped with the sensing components.

The main difficulty in terms of integration and use of carbon dioxide sensors is their limited stability. Due to the fragile equilibrium between the quaternary ammonium ion which serves in a buffering capacity within this system, and the influence of acidic chemicals from the aqueous phase the long-term stability is limited for these systems. Steps towards the improvement of this long-term stability have been made recently at a larger scale by Fritzsche *et al.*,<sup>88</sup> but have yet to be adapted to a microfluidic scale. Calvo-López *et al.*<sup>15</sup> presented a credit card-sized microsystem for the determination of carbon dioxide during wine and beer production, with a linear range of 0.255 to 10 g L<sup>-1</sup> and a detection limit of 83 mg L<sup>-1</sup>. A gas diffusion module was used to transfer the carbon dioxide into a bromothymol blue pH sensitive acceptor solution that was read out at 607 nm with a detection system consisting of an LED and a photodiode integrated in a printed circuit board. Sell *et al.*<sup>79</sup> managed to document the diffusion of carbon dioxide in water and brine by using the fluorescence quenching fluorescein. Liu *et al.*<sup>89</sup> studied the solubility of carbon dioxide in water and brine using confocal Raman spectroscopy. For this purpose the relationship between carbon dioxide solubility and Raman band intensity was fit with a third order polynomial function that depended on the NaCl concentration in the brine. To make carbon dioxide viable, significant effort is required towards the improvement of existing options or investigation of new sensors concepts as the options currently are still very limited.

#### d. Glucose

Glucose sensing has been researched for more than 30 years, in particular for medical diagnostics. Electrochemical and optical methods have been intensively investigated. However, continuous glucose monitoring is still limited and monitoring in large-scale bioreactors is performed at-line with various systems.<sup>90</sup> Overall, many more electrochemical detection methods<sup>91</sup> are in use for glucose monitoring than optical ones. Literature on microfluidic glucose monitoring in microfluidic devices is sparse. A summary of potential routes of

monitoring glucose optically was published by Steiner *et al.*<sup>92</sup> In their comprehensive review, Steiner *et al.* classify glucose sensors in four categories according to the method of glucose recognition: a) monitoring of optical properties of enzymes, their cofactors or cosubstrates; b) measurement of enzymatic oxidation products of glucose oxidase; c) the use of boronic acids and d) the use of Concanavalin A or other glucose binding proteins. All of these methods have proven to be successful in bench scale or larger systems but their translation to the microscale is a challenge. The transfer of glucose sensors based on monitoring of products of the enzymatic conversion of glucose seems to be the most promising in our opinion since miniaturized oxygen and pH sensor are established.

The recently presented glucose sensor by Nacht *et al.*<sup>93</sup> for subcutaneous monitoring of glucose shows that the sensing principle can be transferred to microfluidics. For this application, the layers of luminescent dye and enzyme suspended in polymer matrices were spray-coated onto optical fibers. Another system that seems to be least likely to display a lot of cross sensitivity and has been shown to be suitable for miniaturisation already is the glucose-oxidase (GOx) and horseradish peroxidase (HRP) enzymatic cascade. The use of this principle is shown in a paper by Iwasaki *et al.*<sup>94</sup> where a glucose oxidase-based sensor on a gold electrode was presented. The sensor spots were about 1 mm in diameter each. Moon *et al.*<sup>95</sup> presented a microfluidic glucose sensing system based on the same principle where glucose was metabolised by glucose-oxidase followed by a horseradish peroxidase reaction in the presence of iodophenol in a two-reactor system. The group of Shinar have presented an organic light-emitting diode-based (OLED-based) sensing platform for the detection of glucose<sup>96</sup> using various dyes. For all glucose sensing methods mentioned here it is important to note that the analyte is consumed in the analysis; this should be considered when glucose is a limiting factor, and the effect becomes more relevant the smaller the working volume of the device.

#### e. Temperature

The precise monitoring of temperature can be crucial for many biological applications, but is often also relevant for the correct operation of other sensors which can be affected by a change in the temperature of their environment. A variation of temperature of a few degrees can make a significant difference in the outcome of an experiment and also affect the readout of other sensors in the system. So having a way to monitor the temperature is very important also in microfluidic systems. Hoera *et al.*<sup>97</sup> presented sensor layers made of polyacrylonitrile and a temperature sensitive ruthenium tris phanthroline probe with a thickness of only 0.5–6 μm capable of monitoring temperatures from 25 to 70 °C. Zhou *et al.*<sup>31</sup> presented PDMS stained with ZnO particles (quantum dots) for a whole chip temperature measurement. The phenomenon of surface plasmon resonance was utilized for the thermometry in microbioreactors with high accuracy in small





volumes.<sup>98</sup> Wang *et al.*<sup>99</sup> presented a temperature measuring possibility using PDMS doped with luminescence upconversion nanoparticles (UCNPs) consisting of NaYF<sub>4</sub>:Yb<sub>3</sub><sup>+</sup>Er<sub>3</sub><sup>+</sup> under infrared irradiation which was ratiometrically imaged. With this method they were able to image the entire channel of their reactor. Similarly, Kuriyama *et al.*<sup>100</sup> used two-wavelength Raman imaging to monitor the transient temperature in a microfluidic device. For this purpose the intensity ratio between the simultaneously obtained Raman images taken at the same time at two wavelengths was measured.

#### f. Multi-parameter online monitoring

Optical sensors have large potential for multi-parameter systems because they can easily be integrated separately to each other without affecting each other. However, very few systems have thus far been presented that monitor more than one variable at a time.

Zanzotto *et al.*<sup>23</sup> presented a microbioreactor system featuring both an oxygen and pH sensor for the monitoring of the aeration of microbial cultures using commercially available sensor spots that were embedded in the bottom layer of a circular microfluidic chamber (see Fig. 3, A). Multi-parameter monitoring systems like this are very desirable as they give a lot of insight into complex processes which ultimately allows for a better process control. Lee *et al.*<sup>101</sup> successfully demonstrated pH and dissolved oxygen control, as well as optical density (OD) monitoring for their array of microfluidic devices used for high throughput experiments. This was used for the fermentation of *E. coli*. Another multi-parameter system was realised in a paper from the same group.<sup>67</sup> They developed a microfluidic chemostat and turbidostat to control oxygen, OD and temperature in a continuous cell culture. Most recently, Tahirbegi *et al.*<sup>48</sup> integrated optical pH and oxygen sensors into a pesticide detection platform that used the inhibition of algal respiration to detect the presence of pesticides. The sensors were integrated into a glass chip using crosslinking agents to attach the sensor spots to the surface treated glass. The spots themselves were integrated using a microdispenser.

Ehgartner *et al.* (2016)<sup>7</sup> showed that it is possible to simultaneously monitor oxygen and pH using core-shell nanosensors in a microfluidic flow system. For this purpose lipophilic oxygen and pH nanoparticles were embedded into poly(styrene-*block*-vinylpyrrolidone) nanoparticles. Lin *et al.* (2009)<sup>102</sup> demonstrated the use of oxygen and glucose monitoring for the cultivation of mammalian cells in a PDMS microfluidic device to study the microenvironment of the cells. Mousavi *et al.*<sup>103</sup> reported a device suitable for real-time monitoring of pH and oxygen for microfluidic cell and tissue cultures. Oxygen sensor spots were integrated into a laser-machined PMMA chip closed using double-sided adhesive tape. Phenol red dissolved sensing dye was used to monitor the pH at 560 nm using a UV-Vis microvolume spectrophotometer. A commercially available ruthenium complex was

deposited in the sensor spot and spin-coated over by a thin PDMS layer to avoid direct contact between the dye and the aqueous environment.

In future, we expect to see more multi-parameter systems, which allow for a better understanding of culture- or process conditions through time-resolved profiles. Multi parameter systems enable the early detection of transient shifts in cultures or detection of errors *via* real-time comparison.

## 7. Conclusions and outlook

Optical sensors have advanced significantly over the past decades, and their application range is continuously expanding. Monitoring of relevant cell culture and bioprocess variables has been successfully demonstrated, and the optical read-out makes integration into the typically polymer- and glass-based microfluidic devices for biological and biotechnology applications very attractive. As the field of optical sensors advanced, different dyes and matrices were developed for the detection of the same analyte, increasing the possibilities of sensor integration for a desired application. Sensor integration requires consideration of the various sensor formats, but must be chosen with respect to device geometries, material, and bonding/assembly methods. They also link with detection methods, which in turn depend on device characteristics. In general, it is best to consider what analyte should be detected, and what its expected range or concentration is. Next the sensing principle should be chosen based on available readout equipment and specific application. Depending on those factors a suitable dye, sensor, and device matrix can be chosen and optimized for the specific application, following the iteration scheme shown in Fig. 1. In our experience, this strategy yields the highest chance to achieve a robust and accurate quantification of the targeted analyte.

Sophisticated sensors and detection methods have been developed and miniaturized for common analytes such as oxygen and pH, but there is still a need for development when it comes to other biotechnologically relevant variables. Carbon dioxide sensors require further development both in terms of miniaturization and lifetime, while analytes such as acetate, lactate and ammonia have not been monitored in microfluidic devices though they are relevant for the understanding of cellular metabolism and achieving or maintaining product quality.<sup>104,105</sup> There is also a strong need to develop optical methods for specific compound monitoring in order to enable the detection of target products, such as proteins, biomarkers, and small molecules. This would enable an online quantification of process yields and thus lead to a more comprehensive process understanding.

With further advances of sensor technology, multi-parameter monitoring systems will become more prominent, allowing the quantification of multiple parameters at once, therefore providing a time-resolved fingerprint of the culture and process conditions. More advanced sensor technology will therefore also underpin new applications for microfluidic devices. High throughput screening options will be necessary



for parallel monitoring of multiplexed systems. For small scale use, improvements necessary include the realisation of simpler and more portable systems. This also concerns further miniaturization of detection and liquid handling equipment. To achieve true lab on a chip functionality, all components necessary for successful analyte monitoring will need to be both small and robust. This will then allow the full exploitation of the potential that miniaturization offers for applications in high throughput screening, process optimization, and cell and tissue-based microsystems.

## Acknowledgements

The authors gratefully acknowledge the People Programme (Marie Curie Actions, Multi-ITN) of the European Union's Seventh Framework Programme for research, technological development and demonstration, for funding Pia Gruber's PhD studentship (Grant Number 608104) and the Biotechnology and Biological Sciences Research Council (BBSRC, BB/L000997/1). We thank Micronit GmbH for allowing us to use their image of a microfluidic device for the graphical abstract of this publication. We thank Sulaiman M. Alwahid and Chiara Szita for proof-reading this manuscript.

## References

- D. Lübbbers and N. Opitz, *Sens. Actuators, A*, 1983, **4**, 641–654.
- O. S. Wolfbeis, H. E. Posch and H. W. Kroneis, *Anal. Chem.*, 1985, **57**, 2556–2561.
- C. Demuth, J. Varonier, V. Jossen, R. Eibl and D. Eibl, *Appl. Microbiol. Biotechnol.*, 2016, **100**, 3853–3863.
- X.-D. Wang and O. S. Wolfbeis, *Chem. Soc. Rev.*, 2014, **43**, 3666–3761.
- T. V. Kirk and N. Szita, *Biotechnol. Bioeng.*, 2013, **110**, 1005–1019.
- D. Schäpper, M. Alam, N. Szita, A. Eliasson Lantz and K. Germaey, *Anal. Bioanal. Chem.*, 2009, **395**, 679–695.
- J. Ehgartner, M. Strobl, J. M. Bolivar, D. Rabl, M. Rothbauer, P. Ertl, S. M. Borisov and T. Mayr, *Anal. Chem.*, 2016, **88**, 9796–9804.
- Y. H. Lee and G. T. Tsao, in *Advances in Biochemical Engineering*, Springer, 1979, vol. 13, pp. 35–86.
- J. W. Severinghaus and A. F. Bradley, *J. Appl. Physiol.*, 1958, **13**, 515–520.
- S. A. Pfeiffer and S. Nagl, *Methods Appl. Fluoresc.*, 2015, **3**, 034003.
- S. Sun, B. Ungerböck and T. Mayr, *Methods Appl. Fluoresc.*, 2015, **3**, 034002.
- W. Göpel, *Chemical and biochemical sensors; Pt. 2*, VCH, Weinheim, 1992.
- S. Lee, B. L. Ibey, G. L. Coté and M. V. Pishko, *Sens. Actuators, B*, 2008, **128**, 388–398.
- D. Sud, G. Mehta, K. Mehta, J. Linderman, S. Takayama and M.-A. Mycek, *J. Biomed. Opt.*, 2006, **11**, 050504.
- A. Calvo-López, O. Ymbern, D. Izquierdo and J. Alonso-Chamarro, *Anal. Chim. Acta*, 2016, **931**, 64–69.
- F. Del Ben, M. Turetta, G. Celetti, A. Piruska, M. Bulfoni, D. Cesselli, W. T. Huck and G. Scoles, A Method for Detecting Circulating Tumor Cells Based on the Measurement of Single-Cell Metabolism in Droplet-Based Microfluidics, *Angew. Chem.*, 2016, **128**(30), 8723–8726.
- P. Gruber, M. P. C. Marques, P. Sulzer, R. Wohlgemuth, T. Mayr, F. Baganz and N. Szita, *Biotechnol. J.*, 2017, 1600475, DOI: 10.1002/biot.201600475.
- L. C. Lasave, S. M. Borisov, J. Ehgartner and T. Mayr, *RSC Adv.*, 2015, **5**, 70808–70816.
- S. A. Pfeiffer, S. M. Borisov and S. Nagl, In-line monitoring of pH and oxygen during enzymatic reactions in off-the-shelf all-glass microreactors using integrated luminescent microsensors, *Microchim. Acta*, 2017, **184**(2), 621–626.
- Pyro-Science*, <http://www.pyro-science.com/overview-fiber-optic-oxygen-sensors.html>, 2016.
- PreSens*, <http://www.presens.de/products/brochures/category/sensor-probes/brochure/oxygen-microsensors.html>, 2015.
- Ocean-Optics*, <http://oceanoptics.com/product/ph-bcg-trans/>, 2016.
- A. Zanzotto, N. Szita, P. Boccuzzi, P. Lessard, A. J. Sinskey and K. F. Jensen, *Biotechnol. Bioeng.*, 2004, **87**, 243–254.
- A. Super, N. Jaccard, M. P. Cardoso Marques, R. J. Macown, L. D. Griffin, F. S. Veraitch and N. Szita, *Biotechnol. J.*, 2016, **11**, 1179–1189.
- P. C. Thomas, M. Halter, A. Tona, S. R. Raghavan, A. L. Plant and S. P. Forry, *Anal. Chem.*, 2009, **81**, 9239–9246.
- Colibri-Photonics*, <http://www.colibri-photonics.com/index.php/component/content/article/17>, 2016.
- N. Klauke, P. Monaghan, G. Sinclair, M. Padgett and J. Cooper, *Lab Chip*, 2006, **6**, 788.
- G. Mistlberger, S. M. Borisov and I. Klimant, *Sens. Actuators, B*, 2009, **139**, 174–180.
- B. Ungerböck, S. Fellingner, P. Sulzer, T. Abel and T. Mayr, *Analyst*, 2014, **139**, 2551.
- M. Skolimowski, M. W. Nielsen, J. Emnéus, S. Molin, R. Taboryski, C. Sternberg, M. Dufva and O. Geschke, *Lab Chip*, 2010, **10**, 2162–2169.
- J. Zhou, H. Yan, Y. Zheng and H. Wu, *Adv. Funct. Mater.*, 2009, **19**, 324–329.
- R. Samy, T. Glawdel and C. L. Ren, *Anal. Chem.*, 2008, **80**, 369–375.
- L. Gui and C. L. Ren, *Appl. Phys. Lett.*, 2008, **92**, 024102.
- B. Ungerböck, V. Charwat, P. Ertl and T. Mayr, *Lab Chip*, 2013, **13**, 1593.
- H. Zhu, X. Zhou, F. Su, Y. Tian, S. Ashili, M. R. Holl and D. R. Meldrum, *Sens. Actuators, B*, 2012, **173**, 817–823.
- S. Grist, N. Oyunerdene, J. Flueckiger, J. Kim, P. Wong, L. Chrostowski and K. Cheung, *Analyst*, 2014, **139**, 5718–5727.
- J. P. Metters, R. O. Kadara and C. E. Banks, *Analyst*, 2011, **136**, 1067.
- T. Mayr, T. Abel, B. Ungerböck, M. Sagmeister, V. Charwat, P. Ertl, E. Kraker, S. Köstler, A. Tschepp and B. Lamprecht, Opto-chemical sensors based on integrated ring-shaped organic photodiodes: progress and applications, *Proc. SPIE*, 2012, **8479**, 84790H-1.



- 39 W. Zhan, G. H. Seong and R. M. Crooks, *Anal. Chem.*, 2002, **74**, 4647–4652.
- 40 W.-G. Koh and M. Pishko, *Sens. Actuators, B*, 2005, **106**, 335–342.
- 41 V. Nock, R. J. Blaikie and T. David, *Lab Chip*, 2008, **8**, 1300–1307.
- 42 J. R. Etzkorn, W.-C. Wu, Z. Tian, P. Kim, S.-H. Jang, D. R. Meldrum, A. K. Jen and B. A. Parviz, *J. Micromech. Microeng.*, 2010, **20**, 095017.
- 43 J. Ehgartner, P. Sulzer, T. Burger, A. Kasjanow, D. Bouwes, U. Krühne, I. Klimant and T. Mayr, *Sens. Actuators, B*, 2016, **228**, 748–757.
- 44 K. Rennert, S. Steinborn, M. Gröger, B. Ungerböck, A.-M. Jank, J. Ehgartner, S. Nietzsche, J. Dinger, M. Kiehntopf and H. Funke, *Biomaterials*, 2015, **71**, 119–131.
- 45 C. Herzog, E. Beckert and S. Nagl, *Anal. Chem.*, 2014, **86**, 9533–9539.
- 46 J. R. Etzkorn, W.-C. Wu, Z. Tian, P. Kim, S.-H. Jang, D. R. Meldrum, A. K. Y. Jen and B. A. Parviz, *J. Micromech. Microeng.*, 2010, **20**, 095017.
- 47 J. Li, F. Rossignol and J. Macdonald, *Lab Chip*, 2015, **15**, 2538–2558.
- 48 I. B. Tahirbegi, J. Ehgartner, P. Sulzer, S. Zieger, A. Kasjanow, M. Paradiso, M. Strobl, D. Bouwes and T. Mayr, *Biosens. Bioelectron.*, 2017, **88**, 188–195.
- 49 M. Reichen, A. Super, M. Davies, R. Macown, B. O’Sullivan, T. Kirk, M. Marques, N. Dimov and N. Szita, *Chem. Biochem. Eng. Q.*, 2014, **28**, 189–202.
- 50 E. Tkachenko, E. Gutierrez, M. H. Ginsberg and A. Groisman, *Lab Chip*, 2009, **9**, 1085–1095.
- 51 T. Brevig, U. Krühne, R. A. Kahn, T. Ahl, M. Beyer and L. H. Pedersen, *BMC Biotechnol.*, 2003, **3**, 10.
- 52 C. R. Tamanaha, M. P. Malito, S. P. Mulvaney and L. J. Whitman, *Lab Chip*, 2009, **9**, 1468–1471.
- 53 M. Viefhues, S. Sun, D. Valikhani, B. Nidetzky, E. X. Vrouwe, T. Mayr and J. M. Bolivar, *J. Micromech. Microeng.*, 2017, **27**, 065012.
- 54 *Micronit*, 2015.
- 55 N.-T. Nguyen, *Fundamentals and applications of microfluidics*, Artech House, Boston, MA, 2002.
- 56 Y. Xia and G. M. Whitesides, *Angew. Chem., Int. Ed.*, 1998, **37**, 550–575.
- 57 Y.-Y. Chiang, D. Nikolay and N. Szita, *Chips and Tips*, 2016.
- 58 S. P. Ng, F. E. Wiria and N. B. Tay, *Procedia Eng.*, 2016, **141**, 130–137.
- 59 B. Valeur, *Molecular Fluorescence: Principles and Applications*, Wiley-VCH, Weinheim, 2001, ISBNs: 3-527-29919-X (Hardcover); 3-527-60024-8 (Electronic).
- 60 M. A. Bennet, P. R. Richardson, J. Arlt, A. McCarthy, G. S. Buller and A. C. Jones, *Lab Chip*, 2011, **11**, 3821.
- 61 J. Sytsma, J. Vroom, C. De Grauw and H. Gerritsen, *J. Microsc.*, 1998, **191**, 39–51.
- 62 G. Mehta, K. Mehta, D. Sud, J. W. Song, T. Bersano-Begey, N. Futai, Y. S. Heo, M.-A. Mycek, J. J. Linderman and S. Takayama, *Biomed. Microdevices*, 2007, **9**, 123–134.
- 63 G. Liebsch, I. Klimant, B. Frank, G. Holst and O. S. Wolfbeis, *Appl. Spectrosc.*, 2000, **54**, 548–559.
- 64 T. W. Molter, S. C. McQuaide, M. T. Suchorolski, T. J. Strovas, L. W. Burgess, D. R. Meldrum and M. E. Lidstrom, *Sens. Actuators, B*, 2009, **135**, 678–686.
- 65 C. Boniello, T. Mayr, J. M. Bolivar and B. Nidetzky, *BMC Biotechnol.*, 2012, **12**, 11.
- 66 J. M. Bolivar, T. Consolati, T. Mayr and B. Nidetzky, *Trends Biotechnol.*, 2013, **31**, 194–203.
- 67 K. S. Lee, P. Boccazzi, A. J. Sinskey and R. J. Ram, *Lab Chip*, 2011, **11**, 1730–1739.
- 68 P. Jin, J. Chu, Y. Miao, J. Tan, S. Zhang and W. Zhu, *AIChE J.*, 2013, **59**, 2743–2752.
- 69 S. Grist, J. Schmok, M.-C. Liu, L. Chrostowski and K. Cheung, *Sensors*, 2015, **15**, 20030–20052.
- 70 P. E. Oomen, M. D. Skolimowski and E. Verpoorte, *Lab Chip*, 2016, **16**, 3394–3414.
- 71 J. Cao, S. Nagl, E. Kothe and J. M. Köhler, *Microchim. Acta*, 2015, **182**, 385–394.
- 72 D. Bavli, S. Prill, E. Ezra, G. Levy, M. Cohen, M. Vinken, J. Vanfleteren, M. Jaeger and Y. Nahmias, *Proc. Natl. Acad. Sci. U. S. A.*, 2016, **113**, E2231–E2240.
- 73 M. Horka, S. Sun, A. Ruszczak, P. Garstecki and T. Mayr, *Analytical Chemistry*, 2016.
- 74 B. Ungerböck, A. Pohar, T. Mayr and I. Plazl, *Microfluid. Nanofluid.*, 2013, **14**, 565–574.
- 75 P. Abbyad, P.-L. Tharaux, J.-L. Martin, C. N. Baroud and A. Alexandrou, *Lab Chip*, 2010, **10**, 2505–2512.
- 76 L. Brigo, T. Carofiglio, C. Fregonese, F. Meneguzzi, G. Mistura, M. Natali and U. Tonellato, *Sens. Actuators, B*, 2008, **130**, 477–482.
- 77 A. Funfak, J. Cao, O. S. Wolfbeis, K. Martin and J. M. Köhler, *Microchim. Acta*, 2009, **164**, 279–286.
- 78 E. Poehler, S. A. Pfeiffer, M. Herm, M. Gaebler, B. Busse and S. Nagl, *Anal. Bioanal. Chem.*, 2016, **408**, 2927.
- 79 A. Sell, H. Fadaei, M. Kim and D. Sinton, *Environ. Sci. Technol.*, 2013, **47**, 71–78.
- 80 Y. Zilberman, S. K. Ameri and S. R. Sonkusale, *Sens. Actuators, B*, 2014, **194**, 404–409.
- 81 M. Strobl, T. Rappitsch, S. M. Borisov, T. Mayr and I. Klimant, *Analyst*, 2015, **140**, 7150–7153.
- 82 T. Jokic, S. M. Borisov, R. Saf, D. A. Nielsen, M. Köhl and I. Klimant, *Anal. Chem.*, 2012, **84**, 6723–6730.
- 83 S. Jezierski, D. Belder and S. Nagl, *Chem. Commun.*, 2013, **49**, 904.
- 84 M.-H. Wu, J.-L. Lin, J. Wang and Z. Cui, *Biomed. Microdevices*, 2009, **11**, 265–273.
- 85 X. Muñoz-Berbel, R. Rodríguez-Rodríguez, N. Vigués, S. Demming, J. Mas, S. Büttgenbach, E. Verpoorte, P. Ortiz and A. Llobera, *Lab Chip*, 2013, **13**, 4239–4247.
- 86 J. M. Woodley, R. K. Mitra and M. D. Lilly, *Ann. N. Y. Acad. Sci.*, 1996, **799**, 434–445.
- 87 A. Mills, Q. Chang and N. McMurray, *Anal. Chem.*, 1992, **64**, 1383–1389.
- 88 E. E. Fritzsche, P. Gruber, S. Schutting, J. P. Fischer, M. Strobl, J. D. Müller, S. M. Borisov and I. Klimant, *Analytical Methods*, 2016.
- 89 P. Liu and R. A. Mathies, *Trends Biotechnol.*, 2009, **27**, 572–581.



- 90 H. Weichert and M. Becker, *BMC Proceedings*, 2013, vol. 7(6), p. 1, ISBN 1753-6561.
- 91 Y. Lin, P. Yu, J. Hao, Y. Wang, T. Ohsaka and L. Mao, *Anal. Chem.*, 2014, **86**, 3895–3901.
- 92 M.-S. Steiner, A. Duerkop and O. S. Wolfbeis, *Chem. Soc. Rev.*, 2011, **40**, 4805–4839.
- 93 B. Nacht, C. Larndorfer, S. Sax, S. M. Borisov, M. Hajnsek, F. Sinner, E. J. W. List-Kratochvil and I. Klimant, *Biosens. Bioelectron.*, 2015, **64**, 102–110.
- 94 Y. Iwasaki, T. Tobita, K. Kurihara, T. Horiuchi, K. Suzuki and O. Niwa, *Biosens. Bioelectron.*, 2002, **17**, 783–788.
- 95 B. U. Moon, M. G. de Vries, B. H. C. Westerink and E. Verpoorte, *Sci. China: Chem.*, 2012, **55**, 515–523.
- 96 B. Choudhury, R. Shinar and J. Shinar, *J. Appl. Phys.*, 2004, **96**, 2949.
- 97 C. Hoera, S. Ohla, Z. Shu, E. Beckert, S. Nagl and D. Belder, *Anal. Bioanal. Chem.*, 2015, **407**, 387–396.
- 98 L. Davis and M. Deutsch, 2010, arXiv preprint arXiv:1009.4904.
- 99 Y. Wang, W. Cao, S. Li and W. Wen, *Appl. Phys. Lett.*, 2016, **108**, 051902.
- 100 R. Kuriyama and Y. Sato, *Meas. Sci. Technol.*, 2014, **25**, 095203.
- 101 C.-F. Lin, G.-B. Lee, C.-H. Wang, H.-H. Lee, W.-Y. Liao and T.-C. Chou, *Biosens. Bioelectron.*, 2006, **21**, 1468–1475.
- 102 Z. Lin, T. Cherng-Wen, P. Roy and D. Trau, *Lab Chip*, 2009, **9**, 257–262.
- 103 S. A. Mousavi Shaegh, F. De Ferrari, Y. S. Zhang, M. Nabavinia, N. Bintah Mohammad, J. Ryan, A. Pourmand, E. Laukaitis, R. Banan Sadeghian, A. Nadhman, S. R. Shin, A. S. Nezhad, A. Khademhosseini and M. R. Dokmeci, *Biomicrofluidics*, 2016, **10**, 044111.
- 104 K. Ito and T. Suda, *Nat. Rev. Mol. Cell Biol.*, 2014, **15**, 243–256.
- 105 R. J. Burgess, M. Agathocleous and S. J. Morrison, *J. Intern. Med.*, 2014, **276**, 12–24.
- 106 B. Ungerböck, Integration of Luminescent Chemical Sensors into Miniaturized Devices, *PhD Thesis*, Graz University of Technology, 2014.

